

# Robust PV Degradation Methodology and Application

Dirk C. Jordan, Chris Deline, Sarah R. Kurtz, Gregory M. Kimball, and Mike Anderson

**Abstract**—The degradation rate plays an important role in predicting and assessing the long-term energy generation of photovoltaics (PV) systems. Many methods have been proposed for extracting the degradation rate from operational data of PV systems, but most of the published approaches are susceptible to bias due to inverter clipping, module soiling, temporary outages, seasonality, and sensor degradation. In this paper, we propose a methodology for determining PV degradation leveraging available modeled clear-sky irradiance data rather than site sensor data, and a robust year-over-year rate calculation. We show the method to provide reliable degradation rate estimates even in the case of sensor drift, data shifts, and soiling. Compared with alternate methods, we demonstrate that the proposed method delivers the lowest uncertainty in degradation rate estimates for a fleet of 486 PV systems.

**Index Terms**—Degradation rates, durability, photovoltaic (PV) field performance, PV lifetime, reliability.

## I. INTRODUCTION

THE long-term performance and stability of photovoltaics (PV) modules has great impact on the economics of PV installations. Degradation rates have been summarized by Jordan *et al.* and recently updated [1]. Historically, long-term performance has been expressed as a function of initial energy generation and a longer term degradation rate, resulting in a gradual decline in annual performance. Implicit is the assumption of linear performance loss, though many PV degradation mechanisms exhibit marked nonlinearity [2]. SunPower first proposed to determine a long-term degradation rate applying a year-on-year method (YOY) [3]. Instead of a single degradation rate, a distribution of degradation rates is obtained for a single system, the median of which indicates the overall decline of the system. More recently, the YOY method was shown to have a reduced sensitivity to outliers, snow and soiling events [4].

In this paper, we introduce an additional improvement that avoids errors due to irradiance sensor drift, calibration, soiling, or misalignment. This clear-sky method can be applied

Manuscript received June 9, 2017; revised October 18, 2017; accepted November 26, 2017. This work was supported by the U.S. Department of Energy under Contract DE-AC36-08-GO28308 with the National Renewable Energy Laboratory. (Corresponding author: Dirk C. Jordan.)

D. C. Jordan, C. Deline, and S. R. Kurtz are with the National Renewable Energy Laboratory, Golden, CO 80401 USA (e-mail: dirk.jordan@nrel.gov; chris.deline@nrel.gov; Sarah.Kurtz@nrel.gov).

G. M. Kimball and M. Anderson are with the SunPower Corporation, San Jose, CA 95134 USA (e-mail: gregory.kimball@sunpower.com; michael.anderson@sunpower.com).

Color versions of one or more of the figures in this paper are available online at <http://ieeexplore.ieee.org>.

Digital Object Identifier 10.1109/JPHOTOV.2017.2779779

to any climate and is insensitive to common problems such as irradiance measurement inaccuracy. Furthermore, this technique provides a standard approach to assess the health of PV generation assets.

## II. ANALYSIS METHODOLOGY

Here we define degradation rate as a rate of change, with a negative rate representing a decrease in performance. Computing the degradation rates of PV systems from time-series data requires three primary steps which are described here: normalization, filtering, and data analysis.

### A. Normalization

This step calculates a unitless performance ratio (PR) metric with less variability than raw power production data. PR is typically based on the rated power of the system, the measured PV power, and site irradiance. In this method, we also normalize by temperature to generate a temperature-corrected PR:

$$PR = \frac{P}{P_{\text{STC,rated}} * \frac{G_{\text{POA}}}{G_{\text{ref}}} * (1 + \gamma * [T_{\text{cell}} - T_{\text{ref}}])} \quad (1)$$

where  $P$  is the measured dc or ac power of the PV system in watts,  $P_{\text{STC,rated}}$  is the rated power of the PV system in watts,  $G_{\text{POA}}$  is the plane-of-array irradiance,  $G_{\text{ref}}$  is the reference irradiance 1000 W/m<sup>2</sup>,  $\gamma$  is the maximum power temperature coefficient in relative %/°C,  $T_{\text{cell}}$  is the cell temperature in °C, and  $T_{\text{ref}}$  is the reference temperature in °C. We denote the subscript “STC” for normalization with  $T_{\text{ref}}$  of 25 °C [5] and “PTC” for normalization with  $T_{\text{ref}}$  of 45 °C [6]. Two normalization routines are compared using (1)—a conventional PR calculation ( $PR_{\text{PTC}}$ ), where  $G_{\text{POA}}$  and  $T_{\text{cell}}$  are measured with field sensors, and a clear-sky method ( $PR_{\text{CS}}$ ), where  $G_{\text{POA}}$  and  $T_{\text{cell}}$  are modeled and therefore insensitive to soiling or long-term drift.  $PR_{\text{CS}}$ , or PR relative to clear-sky conditions, requires (1) be modified as follows:

$$PR_{\text{CS}} = \frac{P}{P_{\text{STC,rated}} * \frac{G_{\text{POA,cs}}}{G_{\text{ref}}} * (1 + \gamma * [T_{\text{cell,cs}} - T_{\text{ref}}])} \quad (2)$$

where  $G_{\text{POA,cs}}$  is the modeled clear-sky plane-of-array irradiance and  $T_{\text{cell,cs}}$  is the modeled clear-sky cell temperature.  $PR_{\text{CS}}$  uses a static model of expected power that does not change from one year to the next. Since this model does not account for weather or cloud effects, only clear-sky conditions can be included in the subsequent degradation rate calculation.

The model of clear-sky irradiance was based on PV system configuration data and modeling tools publicly available in PVLIB [7]. The site details required are longitude, latitude, time zone, altitude, and PV system mounting configuration. The ground albedo was assumed to be 20% for all systems in the study. Using atmospheric turbidity derived from Linke turbidity parameters, the Ineichen irradiance model generates global horizontal, direct normal and diffuse horizontal irradiance values [8]. The horizontal irradiance is then transposed to the array plane using PVLIB's King transposition model [7].

The model of clear-sky temperature was based on site location as well as monthly average daytime and nighttime temperatures. Temperature data were obtained in high-resolution image format from NASA Earth Observatory with 0.05° spatial resolution [9]. The source data consisted of monthly long-term average day and night temperatures, which were then interpolated to 15-min data using mean values of a rolling 20-day Gaussian window. The following equation computed the clear-sky ambient temperature:

$$T_{\text{amb,cs}} = \frac{(T_{\text{day}} - T_{\text{night}})}{2} * \cos\left(\frac{h + 8.0}{24} * 2\pi\right) + \frac{(T_{\text{day}} + T_{\text{night}})}{2} \quad (3)$$

where  $T_{\text{day}}$  is the average monthly day temperature in °C,  $T_{\text{night}}$  is the average monthly night temperature in °C, and  $h$  is the time since midnight in hours. The factor 8 in the cosine term is an empirical factor taking into account the lag between daily peak irradiance and temperature. Clear-sky cell temperature for an assumed polymer backsheet and rack-mounted PV system was then derived from the field validation work of King *et al.* using the following relation [10]:

$$T_{\text{cell,cs}} = T_{\text{amb,cs}} + G_{\text{poa,cs}} * e^{-3.56} + \frac{G_{\text{poa,cs}}}{333}. \quad (4)$$

The parameter gamma ( $\gamma$ ) in (1) and (2) is used to capture the differences in thermal behavior between wafer and thin film PV cell materials, and is extracted from the PV module datasheets. Although we expect differences in (4) as a function of PV system mounting and module construction, the precision of the temperature model contributes less uncertainty than the use of long-term average ambient temperature data in place of temperature sensors.

### B. Filtering

The filtering step removes data collected during periods of poor or variable solar resource conditions as well as nonrepresentative or biasing data. First, low irradiance conditions are often associated with nighttime data or with errors due to inverter startup and nonuniform irradiance (see Fig. 1). We have found a low irradiance cutoff of 200 W/m<sup>2</sup> to exclude these start-up issues without removing winter data from high latitude locations. Second, a clear-sky index (csi) filter is used, where csi is the ratio of measured irradiance to modeled clear-sky irradiance. Fig. 1(b) indicates the impact of a window filter of variable width (e.g., +/- 10%) around csi equals to 1. We have evaluated csi filters of width 10% and 20% in this analysis. Third,

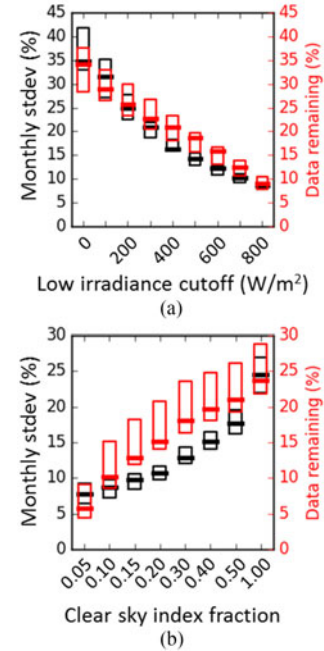


Fig. 1. Monthly standard deviation in  $PR_{CS}$  (left axis) and remaining data (right axis) for ranges of (a) low irradiance cut-off and (b) clear-sky index fraction values.

systems with high dc/ac ratio can be limited during normally high producing days by the input window of the inverter possibly biasing long-term performance assessment. Therefore, we filtered out periods of inverter clipping by excluding data during which power was >99% of the maximum value. Machine-learning algorithms to automatically detect inverter clipping may be useful and incorporated in future work. Finally, an operational filter excluded data outside of a  $\pm 30\%$  band around a 3-month rolling median performance index to identify the rare case where systems are offline for maintenance.

### C. Analysis

The analysis step processes the remaining data to compute a degradation rate based on one of the three methods. In the YOY method, the rate of change is calculated between two points at the same time in subsequent years. Calculating such a rate of change for all data points and all years, results in a histogram of rates of change, the central tendency of which representing the overall system performance. Further details on the methodology can be found in [3] or [4]. In contrast, the standard least square regression (SLS) approach uses all data points in a single regression by minimization of the difference between the model and the data. Finally, the quantile regression is a form of robust regression using quantiles instead of the response mean. [11] Prior to degradation analysis, the normalized, filtered 15-min data are aggregated over a variable time period. Fig. 2(a) shows a decreasing standard deviation of YOY deltas with the number of aggregation days. In general, since long aggregation periods reduce the number of points considered per regression, we found that a 7-day aggregation period delivered satisfactory results. Therefore, unless otherwise stated, 7-day aggregation levels were used in the remainder of the paper.

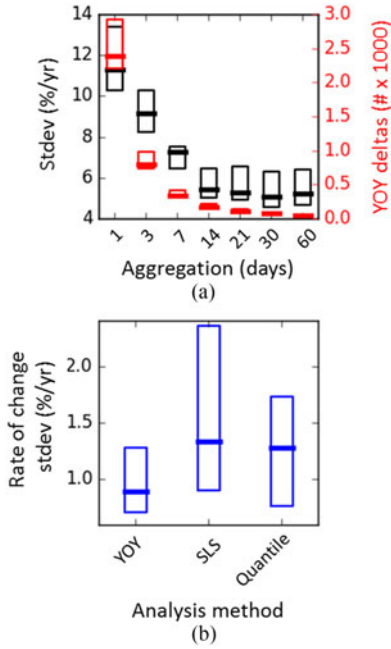


Fig. 2. (a) For the YOY method, increasing the aggregation window results in lower standard deviation in the distribution of year-on-year deltas. (b) The YOY method shows the lowest standard deviation in degradation rates compared with SLS and quantile regression when an inverter is repeatedly analyzed each month.

Fig. 2(b) shows results of the three analysis approaches (YOY, SLS, quantile regression) for the fleet of systems considered in Section IV-B. The YOY method shows the lowest standard deviation in degradation rates compared with SLS and quantile regression, suggesting that the YOY method can yield more consistent degradation estimates.

An example comparison between the two YOY normalization methods is shown for an x-Si PV system at NREL in Fig. 3. The  $PR_{PTC}$  using a calibrated pyranometer is overlaid with the  $PR_{CS}$ . For PV systems with well-maintained pyranometers, both  $PR_{PTC}$  and  $PR_{CS}$  result in approximately the same degradation rate estimate; however, the  $PR_{CS}$  has a higher uncertainty and seasonality for a variety of reasons such as errors in modeled temperature and irradiance and snow on the modules. The analytical method outlined above is also publicly available in “Rd-tools” allowing customization of the above-listed assumptions. [12] For example, the albedo assumption may lead to deviation between the modeled and the measured clear-sky irradiance. As long as the irradiance model is approximately modeling clear sky conditions within this range, we recommend a clear sky index threshold between 10% and 20% to appropriately exclude cloudy, variable irradiance conditions but to allow for potential drift of irradiance sensors.

### III. COMMON EVALUATION QUANDARIES

PV systems with verified irradiance sensor calibration and maintenance are most desirable for long-term performance evaluation, and resulted in a cleaner dataset in Fig. 3. Unfortunately, these conditions are not always met in real-world systems.

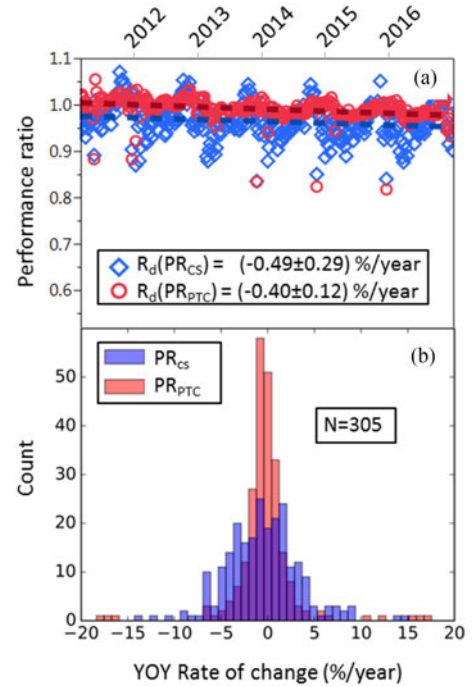


Fig. 3. (a) Performance ratio of a single system at NREL using  $PR_{PTC}$  and  $PR_{CS}$  as a function of time with respective SLS regression lines. (b) Year-on-year aggregated histograms for the respective PR’s. The rate of change values noted in (a) are taken as the medians of the two histograms shown in (b). In addition, the number of data points in the histograms is also given.

#### A. Drifting Irradiance Sensor

The most critical yet often unknown variable is the calibration state of the irradiance sensor. We performed the  $PR_{CS}$  methodology from Section II on the same PV system using different sources of  $G_{poa}$  data. Fig. 4(a) shows the ratio of various  $G_{poa}$  sensors with respect to a regularly calibrated system pyranometer. As a guide to the eye, a no-change line at unity is given by a solid line. The median of ten independently calibrated yet different pyranometers and reference cell one at NREL show flat behavior with respect to the calibrated system pyranometer, indicating no long-term drift within the measurement uncertainty. In contrast, two uncalibrated photodiodes and a second reference cell show marked drift over 5 years at an annualized linear rate of 1%–2%/year, although some sensors drift appears nonlinear.

Fig. 4(b) displays the results using the different sensor and using the  $PR_{PTC}$  and  $PR_{CS}$  metrics. The green bands indicate the  $1\sigma$  standard deviation or 68% confidence interval from a more conventional analysis of ten different methods [13] that include various time-series analyses and independent quarterly  $I-V$  measurements. When the calibrated sensors are used, the degradation rates generally fall into the green band of expected degradation regardless of the PR metric. In contrast, serious deviations can be discerned for the drifting sensors. Using  $PR_{PTC}$  with a drifting  $G_{poa}$  sensor results in grossly incorrect performance assessment, but using  $PR_{CS}$  results in degradation assessment close to the expected range. When using the  $PR_{CS}$  metric, applying a  $\pm 20\%$  csi filter results in degradation rates within the expected range, but applying a  $\pm 10\%$  csi filter

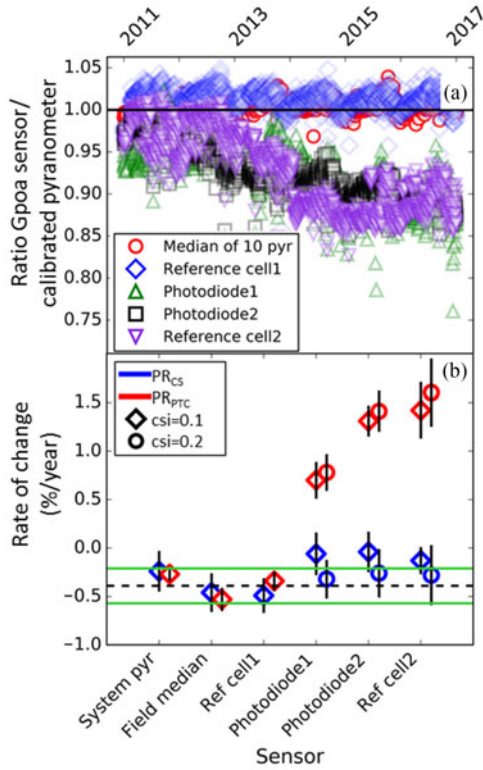


Fig. 4. (a) Ratio of various  $G_{poa}$  sensors with respect to a calibrated reference  $G_{poa}$  pyranometer. Shown are the median of ten pyranometers in the same yard at NREL, two reference cells, and two photodiodes. As guide to the eye, a no-change line is given by a solid line. (b) Rate of change determined using the various  $G_{poa}$  sensors on the same system of Fig. 3(b). The red markers use the respective  $G_{poa}$  sensor while the blue markers use the clear-sky method. The green interval is the band of degradation for this system (see text) and two different csi filters are indicated by different symbols.

results in degradation rates somewhat outside the expected range. In this example, the  $\pm 10\%$  csi filter removes too much data for the heavily degraded sensor and adds positive bias. In the case of severe sensor degradation even as high as  $> 1.5\%/yr$ , the PR<sub>CS</sub> metric allows for accurate assessment of the degradation rate.

### B. Data Shifts

Data shifts are often induced unintentionally in practice by the replacement of hardware or changes in software configuration. For example, the large shift displayed in Fig. 5(a) was caused by the replacement of a dc power sensor. Fig. 6 compares the degradation rate using three different techniques for handling data shifts. The technique of “shift correction” adjusts the data based on the minimization of the root mean square error from a regression. [14] However, this requires knowledge of the degradation curve that is commonly assumed to be linear, but may take on a variety of shapes. The technique of “Removal” uses the YOY approach to highlight and exclude a secondary peak, see Fig. 5(b), caused by the data shift. The technique of “two step” evaluates the data in two steps by separating the sections before and after the shift and then aggregating the YOY deltas into a combined histogram. The SLS regression for the two-step procedure is combined by evaluating the median of the

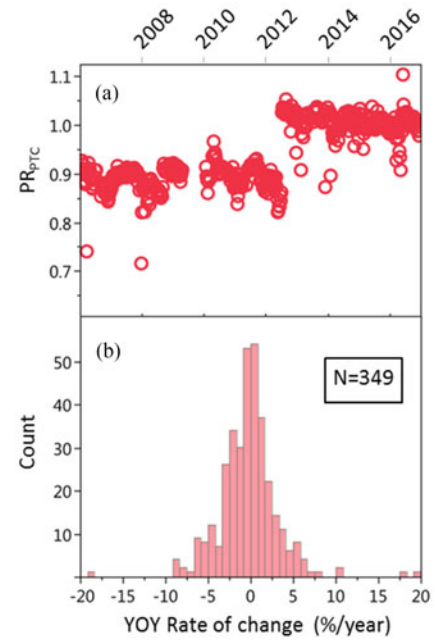


Fig. 5. (a) Data shift occurrence because of a maintenance event of the dc measurement sensor. (b) Resulting secondary peak in the PR<sub>PTC</sub> year-on-year histogram.

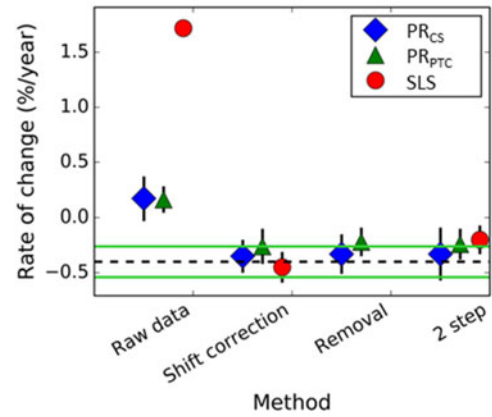


Fig. 6. YOY PRs and SLS for different data shift correction procedures compared with evaluation with the uncorrected data. The green interval is the band of degradation for this system based primarily on ten more conventional time series analyses and independent tests such as  $I-V$  measurements.

two separate degradation rates combined with a pooled standard deviation. Fig. 6 compares the degradation rate using three different data shift correction techniques. The green interval is a band of degradation determined similarly to Section III-A. Because the interval relies mostly on shift correction and regression approaches, the interval should be viewed as an approximate guideline rather than an accurate confidence interval of the system performance. The greatest sensitivity to the data shift of the uncorrected data is shown by the SLS. Although the YOY approaches are biased by the data shift, the sensitivity is far less compared with SLS. Because the removal method requires the application of the YOY method, the SLS is not applicable and therefore absent from the “Removal” dataset in Fig. 6. Within the uncertainty, the data shift correction methods appear to be

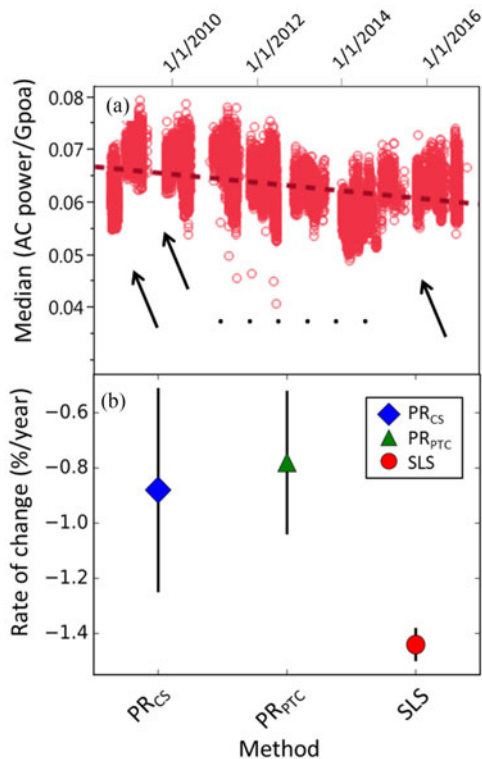


Fig. 7. (a) PV system in southern California exhibiting substantial seasonal soiling intervals some marked by arrows. (b) Results of the YOY approach compared with a SLS regression approach.

approximately equivalent for the performance metrics although the YOY methods appear perhaps slightly more consistent. In reality, most data shifts are not as pronounced and easily detectable as in this example, in which case the sensitivity of the SLS regression can be of considerable concern.

### C. Soiling

Soiling has seen an increased interest in recent years because of its significant impact on the project economics in some locations. Fig. 7 shows the ac power from a PV system in southern California that exhibits considerable soiling intervals, some of which are indicated by arrows. Reversible performance changes can introduce bias into degradation analysis. Linear methods such as SLS regression or quantile regression are particularly sensitive to bias resulting from anomalous performance at the beginning or end of the evaluation period, which is known in statistics as high leverage. In addition, SLS methods are sensitive to bias due to the largest reversible fluctuations caused by soiling.

To obtain an unbiased performance assessment with linear methods, the soiling events would have to be carefully removed from time-series data requiring detailed knowledge from a soiling station, where one module, for example, is permitted to natural soil, while another one is cleaned on a regular basis. Fig. 7 highlights the importance of using YOY methods instead of linear regression to analyze time-series data that has been affected by soiling. Applying the YOY approach for both PR methods reduces error associated with soiling, see Fig. 7(b),

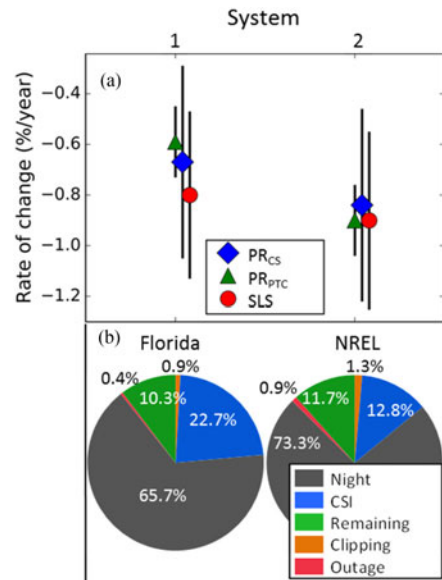


Fig. 8. (a) Two PV systems located near Pensacola, Florida that showed more partly cloudy days. (b) Data percentage impact of the described filters for the Florida systems and a comparable system at NREL.

especially seasonally occurring soiling trends, as shown before [4].

### D. Cloudy Climates

With the emphasis on clear-sky conditions, it is important to demonstrate how the proposed method performs in locations where cloudy conditions occur more often. Significant installed PV capacity and frequent partly cloudy conditions in Florida make this an excellent region for demonstrating the effectiveness of the methods in lower irradiance climates, as displayed in the inset of Fig. 8(a). We applied the proposed method to two systems on a school building near Pensacola, FL, that some of the authors evaluated in 2012. Fig. 8(a) shows that the proposed method resulted in very good agreement with the more traditional time-series approach of the earlier evaluation [15]. In addition, we provide the data percentage impact of the described filters for the systems in Florida in comparison with a similar system at NREL during the same 4.5 years of operation. None of the systems experienced major operational outages or significant inverter clipping. It should be noted that these pie charts may differ depending on location, design, operational consistency, and data quality. The majority of the data is removed due to low irradiance or night time filter. The number of remaining data points and the impact of the outage and clipping filter are approximately the same for both systems. Even with the cloudier conditions leading to greater csi filtering, the Florida system still had sufficient remaining data to enable successful analysis. However, longer evaluation periods may be required as the cloudiness increases.

### E. Nonlinearities

The implicit assumption in the analysis above is the linearity of the long-term degradation curve. However, PV degradation

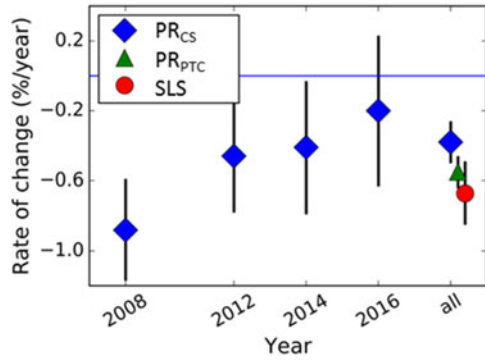


Fig. 9. Nonlinear trend for a heterojunction crystalline silicon (x-Si) system using the  $PR_{CS}$  metric. The time series is evaluated in 2 year increments along with cumulative total degradation rates using multiple performance metrics.

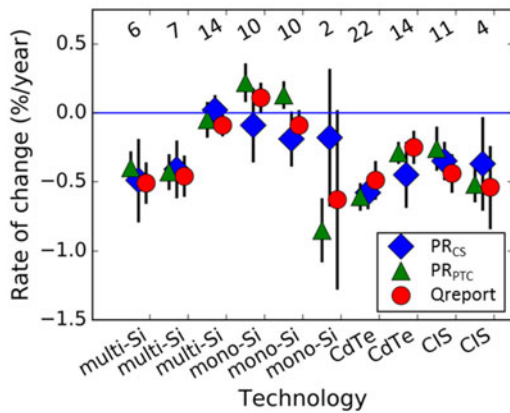


Fig. 10. Comparison of the various systems at NREL using the year-on-year approach using  $PR_{CS}$  and  $PR_{PTC}$  contrasted to a quarterly report (Qreport) that consists of ten more conventional time-series analysis and independent tests such as  $I-V$  measurements. The number above each system indicates the systems' age in years.

may not be linear over the life of the system. Depending on the underlying degradation mechanisms, the degradation curve of a PV system may exhibit substantial deviation from linearity [2]. In the case of suspected nonlinearity, the entire datasets can be divided into shorter sections, as illustrated in Fig. 9. This system, which was installed at the end of 2007, exhibited a higher degradation in the first 2 years than in subsequent years using  $PR_{CS}$ , which was aggregated in 7 days [16]. Because of field upgrades, during which time the system was not field exposed, a gap on the time axis is present. In addition, the degradation rates for the entire dataset using different performance metrics are also displayed. Even as the uncertainties for the 3 metrics overlap, the YOY methods show a degradation rate that is closer to the year 3–9 behavior than the SLS regression.

#### IV. APPLICATIONS

##### A. Validation With NREL PV Systems

NREL maintains an array of PV systems representing many PV module technologies and an operating history  $>10$  years. In addition to continuous monitoring, the PV systems are characterized by periodic  $I-V$  curve measurements, infrared imaging, and visual inspection. NREL prepares quarterly reports on the

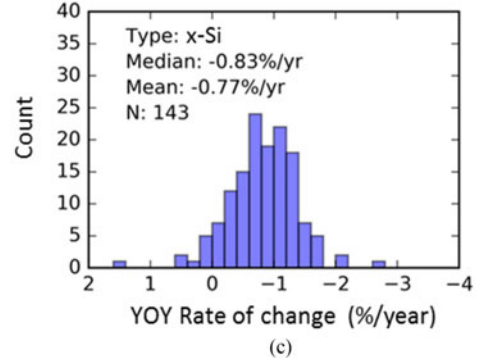
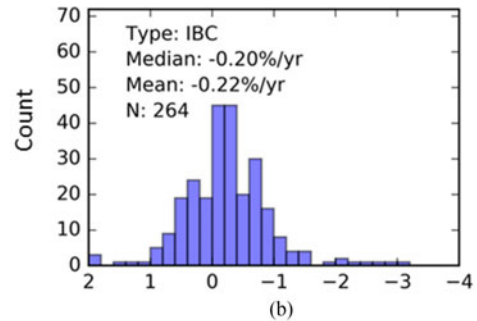
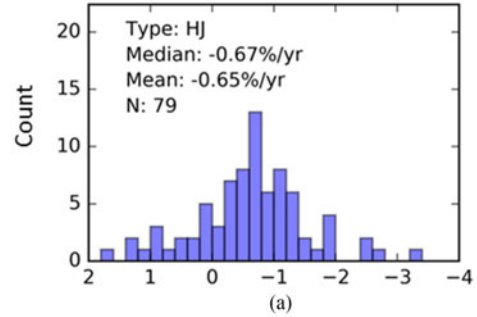


Fig. 11. Aggregated degradation rates derived from the  $PR_{CS}$  YOY method for a fleet of systems partitioned by technology, (a) heterojunction, (b) interdigitated backcontact, (c) and all other x-Si.

performance of each PV system based on time-series analysis using a variety of methods. The results of the most recent report were compared with the results of a new study based on  $PR_{CS}$  and  $PR_{PTC}$  normalization and YOY analysis. Fig. 10 shows good agreement between the methods used in the quarterly report and the methods outlined in Section II.

##### B. PV Fleet Roll-Up

The  $PR_{CS}$  clear-sky method described in Section II was applied to PV electricity-production data from a group of 486 inverters to demonstrate the wide applicability of the method. The analysis was performed by SunPower using software tools shared between NREL and SunPower. The PV systems were commissioned between 2006 and 2011, with a mean operating age of 7.3 years and total STC capacity of 230 MW. The data represent one of the largest sets of PV system time-series analysis in the literature, and the minimum age of 6 years reduces the impact of LID and other short-term stabilization effects. The data presented in [17] overlap in part with the data presented in Fig. 11, with a critical difference that in this paper clear sky

models of sensor values are used instead of raw measured sensor data for normalizing PV power. As PV systems age, they are more likely to accumulate outages or degradation in irradiance or temperature sensors, so the methods presented in Section II are expected to grow in importance as time-series data on older systems become available. Degradation analysis was performed for each PV system, and statistics were computed for the population of PV systems based on the module technology (see Fig 11). The median degradation rate for PV systems with heterojunction (HJ) modules is similar to a more detailed HJ system investigation by Jordan *et al.*[16], while the fleet of interdigitated back contact (IBC) modules showed a statistically significant lower rate of change than the HJ and the fleet of other crystalline silicon (x-Si) systems. Distilling further statistically significant trends was difficult because of the convolution of the time series, technology, temperature, and mounting differences and awaits further investigation.

## V. CONCLUSION

We present a robust methodology for estimating the degradation rate of PV systems by combining the YOY method with clear-sky modeling. The clear-sky normalization step prevents bias due to poor maintenance or irregular calibration of irradiance and temperature sensors. The filtering approach mitigates bias due to inverter clipping and temporary outages as well as noise due to nonuniform irradiance. The YOY analysis limits the impact of data shifts, soiling, and nonlinearity as compared with linear methods. When analyzing high-quality data from PV systems at NREL, the proposed methodology yielded similar degradation rate estimates to those published previously. Applying the robust methodology to a fleet of PV systems, we were able to discriminate between the long-term degradation behavior of different technologies including HJ and IBC.

## ACKNOWLEDGMENT

The authors would like to thank A. Shinn, A. Nag, M. Deceglie, B. Bourne, K. Davis, NREL's reliability and measurement group.

## REFERENCES

- [1] D. C. Jordan, S. R. Kurtz, K. T. VanSant, and J. Newmiller, "Compendium of photovoltaic degradation rates," *Prog. Photovolt. Res. Appl.*, vol. 24, no. 7, pp. 978–989, 2016, doi:[10.1002/pip.2744](https://doi.org/10.1002/pip.2744).
- [2] D. C. Jordan, T. J. Silverman, B. Sekulic, and S. R. Kurtz, "PV degradation curves: Non-linearities and failure modes," *Prog. Photovolt. Res. Appl.*, vol. 25, pp. 583–591, 2016, doi:[10.1002/pip.2835](https://doi.org/10.1002/pip.2835).
- [3] E. Hasselbrink *et al.*, "Validation of the PVLife model using 3 million module-years of live site data," in *Proc. 39th IEEE Photovolt. Spec. Conf.*, Tampa, FL, USA, 2013, pp. 7–13, doi:[10.1109/PVSC.2013.6744087](https://doi.org/10.1109/PVSC.2013.6744087).
- [4] D. C. Jordan, M. G. Deceglie, and S. R. Kurtz, "PV degradation methodology comparison — A basis for a standard," in *Proc. 43rd IEEE Photovolt. Spec. Conf.*, Portland, OR, USA, 2016, pp. 0273–0278, doi:[10.1109/PVSC.2016.7749593](https://doi.org/10.1109/PVSC.2016.7749593).
- [5] STC: Irradiance = 1000 W/m<sup>2</sup>, Air mass = 1.5, Module temperature = 25 °C.
- [6] T. Dierauf, A. Growitz, S. Kurtz, J. L. Becerra Cruz, E. Riley, and C. Hansen, "Weather-corrected performance ratio," Nat. Renewable Energy Lab., Golden, CO, USA, Tech. Rep. NREL/TP-5200-57991, Apr. 2013.
- [7] J. S. Stein, W. F. Holmgren, J. Forbess, and C. W. Hansen, "PVLIB: Open source photovoltaic performance modeling functions for Matlab and Python," in *Proc. 43rd IEEE Photovolt. Spec. Conf.*, Portland, OR, USA, 2016, pp. 3425–3430.
- [8] P. Ineichen and R. Perez, "A New airmass independent formulation for the Linke turbidity coefficient," *Sol. Energy*, vol. 73, pp. 151–157, 2002.
- [9] [Online]. Available: [https://neo.sci.gsfc.nasa.gov/view.php?datasetId=MOD\\_LSTD\\_CLIM\\_M](https://neo.sci.gsfc.nasa.gov/view.php?datasetId=MOD_LSTD_CLIM_M)
- [10] D. L. King, J. A. Kratochvil, and W. E. Boyson, *Photovoltaic Array Performance Model*. Albuquerque, NM, USA: Sandia Nat. Lab., Aug. 2004.
- [11] R. Koenker and G. J. Bassett, "Regression quantiles," *Econometrica*, vol. 46, no. 1, pp. 33–50, 1978.
- [12] 2017. [Online]. Available: <https://github.com/NREL/rdtools>
- [13] D. C. Jordan and S. R. Kurtz, "Thin-film reliability trends toward improved stability," in *Proc. 37th IEEE Photovolt. Spec. Conf.*, Seattle, WA, USA, 2011, pp. 000827–000832, doi:[10.1109/PVSC.2011.6186081](https://doi.org/10.1109/PVSC.2011.6186081).
- [14] D. C. Jordan and S. R. Kurtz, "Analytical improvements in PV degradation rate determination," in *Proc. 35th IEEE Photovolt. Spec. Conf.*, Honolulu, HI, USA, 2010, pp. 002688–002693.
- [15] K. O. Davis, S. R. Kurtz, D. C. Jordan, J. H. Wohlgemuth, and N. Sorloaica-Hickman, "Multi-pronged analysis of degradation rates of photovoltaic modules and arrays deployed in Florida," *Prog. Photovolt. Res. Appl.*, vol. 21, pp. 702–712, 2012.
- [16] D. C. Jordan *et al.*, "Silicon heterostructure PV system field performance," in *Proc. 44th IEEE Photovolt. Spec. Conf.*, Washington DC, USA, 2017, pp. 1–6.
- [17] A. J. Curran *et al.*, "Determining the power rate of change of 353 plant inverters time-series data across multiple climate zones, using a month-by-month data science analysis," in *Proc. 44th IEEE Photovolt. Spec. Conf.*, Washington, DC, USA, 2017.

Authors' photographs and biographies not available at the time of publication.